

$K^0 - \bar{K}^0$ mixing in the minimal flavor-violating two-Higgs-doublet models

Natthawin Cho^{1*} Xin-Qiang Li^{1†} Fang Su^{1‡} Xin Zhang^{1§}

¹ Institute of Particle Physics and Key Laboratory of Quark and Lepton Physics (MOE),
Central China Normal University, Wuhan, Hubei 430079, China

May 15, 2022

Abstract

The two-Higgs-doublet model (2HDM), as one of the simplest extensions of the Standard Model (SM), is obtained by adding another scalar doublet to the SM, which could affect many low-energy processes. Under the criterion of minimal flavor violation, the other one is fixed to be either color-singlet or color-octet, which are named as the type-III and the type-C 2HDM, respectively. In this paper, we study the charged-scalar effects of these two models on the $K^0 - \bar{K}^0$ mixing, an ideal process to probe New Physics (NP) beyond the SM. Firstly, we perform a complete one-loop computation of the box diagrams relevant to the $K^0 - \bar{K}^0$ mixing, keeping the mass and momentum of the external strange quark up to the second order. Together with the up-to-date theoretical inputs, we then give a detailed phenomenological analysis, in the cases of both real and complex Yukawa couplings of the charged scalars to quarks. The parameter spaces allowed by the current experimental data on the mass difference Δm_K and the CP-violating parameter ϵ_K are obtained and the differences between these two 2HDMs are investigated, which are helpful to distinguish them from each other from a phenomenological point of view.

*natthawin.cho@mails.ccnucnu.edu.cn

†xqli@itp.ac.cn

‡sufang@itp.ac.cn

§zhangxin027@mails.ccnucnu.edu.cn

1 Introduction

The SM of particle physics has been proved to be successful because of its elegance and predictive capability. Almost all predictions in the SM are in good agreement with the experimental measurements, especially for the discovery of Higgs boson with its mass around 125 GeV [1, 2]. The discovery of Higgs suggests that the electro-weak symmetry breaking (EWSB) is probably realized by the Higgs mechanism implemented via a single scalar doublet. However, the EWSB is not necessarily induced by just one scalar. What's interesting is that a lot of NP models are equipped with an extended scalar sector, for example, the minimal supersymmetric standard model (MSSM) requires at least two Higgs doublets [3]. Moreover, the SM does not have enough sources for CP violation to generate sufficient size of baryon asymmetry of the universe (BAU) [4, 5, 6].

One of the simplest extensions of the SM scalar sector is the so-called 2HDM [7], in which a second scalar doublet is added to the SM field content. The added Higgs doublet can provide additional sources of CP violation besides the Cabibbo-Kobayashi-Maskawa (CKM) [8, 9] matrix, making it possible to explain the BAU [4].

To avoid the experimental constraints on the flavor-changing neutral currents (FCNCs), which are forbidden at tree level, due to Glashow-Iliopoulos-Maiani (GIM) mechanism [10], and are highly suppressed at loop level in the SM, appear even at tree level. The natural flavor conservation (NFC) [11] and minimal flavor violation (MFV) hypotheses [12, 13, 14, 15] have been proposed. In the NFC hypothesis, the absence of dangerous FCNCs is guaranteed by limiting the number of scalar doublets coupling to a given type of right-handed fermion to be at most one. This can be explicitly achieved by applying a discrete \mathbb{Z}_2 symmetry on the two scalar doublets differently, leading to four types of 2HDM (usually called as type-I, II, X and Y) [16, 17], which has been studied extensively for many years [16, 17]. In the MFV hypothesis, to control the flavor-violating interactions, all the scalar Yukawa couplings are assumed to be composed of the SM ones Y^U and Y^D . In the “Higgs basis” [18], in which only one doublet gets a nonzero vacuum expectation value (VEV) and behaves as the SM one, the allowed $SU(3) \times SU(2) \times U(1)$ representation of the second scalar doublet is fixed to be either $(1, 2)_{1/2}$ or $(8, 2)_{1/2}$ [19], which implies that the second scalar doublet can be either color-singlet or color-octet. For convenience, they are referred as type-III and type-C model [20], respectively.

Examples of the color-singlet case include the aligned 2HDM (A2HDM) [21] and the four types of 2HDM reviewed in Refs. [16, 17]. In the color-octet case, the scalar spectrum contains a CP-even, color-singlet Higgs boson (the usual SM one) and three color-octet particles, one CP-even, one CP-odd and one electrically charged [19].

Although the scalar-mediated flavor-violating interactions are protected by the MFV hypothesis, the type-III and type-C models still bring in very interesting phenomena in some low-energy processes, especially due to the presence of a charged Higgs boson [19, 20, 22, 23, 24, 25, 26]. $B_s^0 - \bar{B}_s^0$ mixing has been studied in Ref. [22], in this literature, we explore the $K^0 - \bar{K}^0$ mixing within these two models and pursue possible differences between their effects. As the charged Higgs contributions to the process at the same order as does the W boson in the SM, the NP effects might be significant.

Our paper is organized as follows. In Sec. 2, we review the 2HDMs under the MFV hypothesis briefly and consider the effective Hamiltonian for the $K^0 - \bar{K}^0$ mixing process. In Sec. 3, we perform a complete one-loop computation of the electro-weak corrections to the Wilson coefficients for the $K^0 - \bar{K}^0$ mixing process within the two models. In Sec. 4, the numerical results and discussions are presented in detail. Finally, our conclusions are made in Sec. 5. Explicit expressions for the loop functions appearing in the $K^0 - \bar{K}^0$ mixing are collected in the appendix.

2 Theoretical framework

2.1 Yukawa Sector

The Lagrangian of Yukawa coupling between the two Higgs doublets, Φ_1 and Φ_2 , and quarks in Higgs basis, where only one doublet gets the VEV, can be written as [19, 20]

$$-\mathcal{L}_Y = \bar{q}_L^0 \tilde{\Phi}_1 Y^U u_R^0 + \bar{q}_L^0 \Phi_1 Y^D d_R^0 + \bar{q}_L^0 \tilde{\Phi}_2^{(a)} T_R^{(a)} \bar{Y}^U u_R^0 + \bar{q}_L^0 \Phi_2^{(a)} T_R^{(a)} \bar{Y}^D d_R^0 + \text{h.c.}, \quad (1)$$

$$\tilde{\Phi}_j = i\sigma_2 \Phi_j^*, \quad j = 1, 2, \quad (2)$$

where \bar{q}_L^0 , u_R^0 , and d_R^0 are quark fields and the superscript ‘0’ means that these fields are in the interaction basis. $T_R^{(a)}$ is the $SU(3)$ color generator which determines the color nature of the

second Higgs doublet¹. $Y^{U,D}$ and $\bar{Y}^{U,D}$ are Yukawa couplings and are generally complex 3×3 matrices in the quark flavor space and σ_2 is the Pauli matrix.

According to the MFV hypothesis, the transformation properties of the Yukawa coupling matrices $Y^{U,D}$ and $\bar{Y}^{U,D}$ under the quark flavor symmetry group $SU(3)_{Q_L} \otimes SU(3)_{U_R} \otimes SU(3)_{D_R}$ are required to be the same. This can be achieved by requiring $\bar{Y}^{U,D}$ to be composed of pairs of $Y^{U,D}$ [20]

$$\begin{aligned}\bar{Y}^U &= A_u^* (1 + \epsilon_u^* Y^U Y^{U\dagger} + \dots) Y^U, \\ \bar{Y}^D &= A_d (1 + \epsilon_d Y^U Y^{U\dagger} + \dots) Y^D.\end{aligned}\tag{3}$$

Transforming the Lagrangian in Eq. (1) from the interaction basis to the mass basis, one can obtain the Yukawa interactions of charged Higgs bosons with quarks in the mass-eigenstate basis [20, 22]

$$\mathcal{L}_{H^\pm} = \frac{g}{\sqrt{2}m_W} \sum_{i,j=1}^3 \bar{u}_i T_R^{(a)} (A_u^i m_{u_i} P_L - A_d^i m_{d_j} P_R) V_{ij} d_j H_{(a)}^\pm + \text{h.c.},\tag{4}$$

where $A_{u,d}^i$ are family-dependent Yukawa coupling constants [27]

$$A_{u,d}^i = A_{u,d} \left(1 + \epsilon_{u,d} \frac{m_t^2}{v^2} \delta_{i3} \right),\tag{5}$$

where $v = \langle \Phi_1^0 \rangle = 174$ GeV. In our calculation, we consider the family universal coupling case in which the family-dependent Yukawa couplings, $A_{u,d}^i$, can be simplified to $A_{u,d}^i = A_{u,d}$.

2.2 K^0 - \bar{K}^0 mixing

In the SM and the 2HDMs with MFV, neutral kaon mixing occurs via the box diagrams in Fig. 1². As the Ref. [29] said, the correction from the external momenta is not negligible in K^0 - \bar{K}^0 mixing, so unlike the traditional calculations, we keep the external momentum of s quark to the second order, and we also have to keep its mass to the same order to obtain the gauge-independent result. We can get the effective Hamiltonian as

¹The second Higgs doublet can be either color-singlet or color-octet depends on which type of 2HDM we are considering.

²These diagrams have been obtained by *TikZ-Feynman* [28].

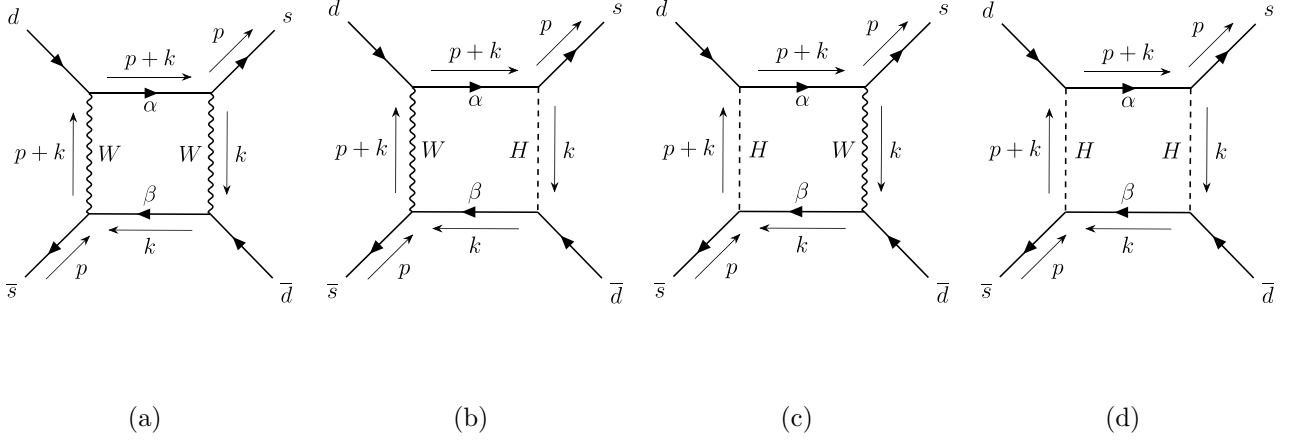


Figure 1: Kaon mixing box diagrams in the SM and the 2HDM.

$$\mathcal{H}_{\text{eff}}^{\Delta F=2} = \frac{G_F^2 m_W^2}{4\pi^2} [C^{VLL}(\mu)Q^{VLL} + C^{SLL}(\mu)Q^{SLL} + C^{TLL}(\mu)Q^{TLL}], \quad (6)$$

where G_F is the Fermi coupling constant, m_W is the mass of W boson, and $C_i(\mu)$ are the scale-dependent Wilson coefficients of the four-quark operators Q_i , which are defined, respectively, as³

$$\begin{aligned} Q^{VLL} &= \bar{s}^\alpha \gamma_\mu (1 - \gamma_5) d^\alpha \bar{s}^\beta \gamma^\mu (1 - \gamma_5) d^\beta, \\ Q^{SLL} &= \bar{s}^\alpha (1 - \gamma_5) d^\alpha \bar{s}^\beta (1 - \gamma_5) d^\beta, \\ Q^{TLL} &= \bar{s}^\alpha \sigma_{\mu\nu} (1 - \gamma_5) d^\alpha \bar{s}^\beta \sigma^{\mu\nu} (1 - \gamma_5) d^\beta, \end{aligned} \quad (7)$$

where α and β are color indices and $\sigma_{\mu\nu} = \frac{1}{2}[\gamma_\mu, \gamma_\nu]$. Note that the above equations do not include the QCD correction effect, which will be considered only in the SM case. The hadronic matrix elements of these operators can be written as [30]

$$\begin{aligned} \langle \bar{K}^0 | Q^{VLL} | K^0 \rangle &= \frac{1}{3} m_K F_K^2 B_1^{VLL}(\mu), \\ \langle \bar{K}^0 | Q^{SLL} | K^0 \rangle &= -\frac{5}{24} R(\mu) m_K F_K^2 B_1^{SLL}(\mu), \\ \langle \bar{K}^0 | Q^{TLL} | K^0 \rangle &= -\frac{1}{2} R(\mu) m_K F_K^2 B_2^{SLL}(\mu), \end{aligned} \quad (8)$$

where m_K is the mass of K^0 meson, F_K is kaon decay constant, $B_i^j(\mu)$ are the scale-dependent bag parameters and $R(\mu)$ is defined as [30]

$$R(\mu) = \left(\frac{m_K}{m_s(\mu) + m_d(\mu)} \right)^2. \quad (9)$$

³There are totally 8 four-quark operators but we have written out only the operators that exist in our calculation.

For the Wilson coefficients, $C^i(\mu)$, the contributions from the SM and the 2HDM cannot be summed directly because their initial scales are different, μ_W for the SM and μ_{H^\pm} for the 2HDM in particular. The scale must be run down to the lattice scale, which is 3 GeV in this work, in order to sum these contributions as in Eq. (39). The explicit expressions of the Wilson coefficients will be shown in Sec. 3.

In neutral kaon mixing process, there are two observables which can be calculated from the effective Hamiltonian in Eq. (6)[30]

$$\Delta m_K = 2\text{Re} \langle \bar{K}^0 | \mathcal{H}_{\text{eff}} | K^0 \rangle, \quad (10)$$

$$\epsilon_K = \frac{\exp(i\pi/4)}{\sqrt{2}\Delta m_K} \text{Im} \langle \bar{K}^0 | \mathcal{H}_{\text{eff}} | K^0 \rangle. \quad (11)$$

The above equations are the general formulae for these two observables. Note that, however, the contribution to Δm_K and ϵ_K consists of short-distance (SD) and long-distance (LD) contribution. Hence, the above equations need some modifications to include the LD contribution. The contribution to Δm_K can be decomposed as [31]

$$\Delta m_K = \Delta m_K^{SD} + \Delta m_K^{LD}|_{\pi\pi} + \Delta m_K^{LD}|_{\eta'}, \quad (12)$$

where [31]

$$\Delta m_K^{LD}|_{\pi\pi} = 0.4\Delta m_K^{\text{exp}}, \quad \Delta m_K^{LD}|_{\eta'} = -0.3\Delta m_K^{\text{exp}}. \quad (13)$$

The SD part of Δm_K can be derived via Eq.(10) with the effective Hamiltonian obtained from box diagrams. For the LD part, we can summarize from Eq.(13) that the contribution to Δm_K is about 10% of the experimental value. However, we still do not understand the contribution from the LD part to Δm_K very well. Hence, we give a result with the LD contribution in the SM case but we do not consider this part in the NP. The formula of ϵ_K with LD contribution is given as [32]

$$\epsilon_K = \frac{\kappa_\epsilon e^{i\phi_\epsilon}}{\sqrt{2}} \frac{\text{Im} M_{12}^{SD}}{\Delta m_K^{\text{exp}}}, \quad (14)$$

where $\kappa_\epsilon = 0.94(2)$ [31], $\phi_\epsilon = 43.52(5)^\circ$ [33] and M_{12}^{SD} is equivalent to $\langle \bar{K}^0 | \mathcal{H}_{\text{eff}} | K^0 \rangle$ with the effective Hamiltonian obtained from box diagrams. The LD contribution to ϵ_K has been included in these two parameters already. In the case of SD contribution, we set κ_ϵ to 1 and ϕ_ϵ to $\pi/4$, which goes back to Eq.(11).

3 Analytic results

3.1 Result in SM

For the SM case, we calculate the Wilson coefficients from the box diagram in Fig. 1 (a) without QCD correction written as

$$C_{SM}^{VLL}(\mu_W) = [\lambda_c^2 S_0(x_c) + \lambda_t^2 S_0(x_t) + 2\lambda_c \lambda_t S_0(x_c, x_t)] \\ + x_s [\lambda_c^2 f_1(x_c) + \lambda_t^2 f_1(x_t) + 2\lambda_c \lambda_t f_1(x_c, x_t)], \quad (15)$$

$$C_{SM}^{SLL}(\mu_W) = x_s [\lambda_c^2 f_2(x_c) + \lambda_t^2 f_2(x_t) + 2\lambda_c \lambda_t f_2(x_c, x_t)], \quad (16)$$

$$C_{SM}^{TLL}(\mu_W) = x_s [\lambda_c^2 f_3(x_c) + \lambda_t^2 f_3(x_t) + 2\lambda_c \lambda_t f_3(x_c, x_t)], \quad (17)$$

where $x_i = \frac{m_i^2(\mu)}{m_W^2}$ and S_0 is the Inami-Lim function [34] which is given by Eq. (A1) in the appendix. The f_i functions are also given in the appendix. Note that we also get the contributions from the Wilson coefficients C_{SM}^{SLL} and C_{SM}^{TLL} in the SM case.

The QCD corrections can be described by the factors η_{cc} , η_{ct} and η_{tt} , which have been calculated to the next-to-next-to-leading order (NNLO) in the literature [31, 35, 36] and have been collected in Ref. [37]. Combining the RG evolution with the QCD corrections, we get

$$\langle \bar{K}^0 | \mathcal{H}_{\text{eff}} | K^0 \rangle_{SM}^{VLL} = \zeta \left[\hat{B} \left(\lambda_c^2 \eta_{cc} S_0(\bar{x}_c) + \lambda_t^2 \eta_{tt} S_0(\bar{x}_t) + 2\lambda_c \lambda_t \eta_{ct} S_0(\bar{x}_c, \bar{x}_t) \right) \right. \\ \left. + P_{SM}^{VLL} x_{s,\mu_W} \left(\lambda_c^2 f_1(x_{c,\mu_W}) + \lambda_t^2 f_1(x_{t,\mu_W}) + 2\lambda_c \lambda_t f_1(x_{c,\mu_W}, x_{t,\mu_W}) \right) \right], \quad (18)$$

$$\langle \bar{K}^0 | \mathcal{H}_{\text{eff}} | K^0 \rangle_{SM}^{SLL} = \zeta \left[P_{SM}^{SLL} C_{SM}^{SLL}(\mu_W) \right], \quad (19)$$

$$\langle \bar{K}^0 | \mathcal{H}_{\text{eff}} | K^0 \rangle_{SM}^{TLL} = \zeta \left[P_{SM}^{TLL} C_{SM}^{TLL}(\mu_W) \right], \quad (20)$$

where $\zeta = \frac{G_F^2 m_W^2 m_K F_K^2}{12\pi^2}$, $\bar{x}_i \equiv \left(\frac{m_i(m_i)}{m_W} \right)^2$ is scale-independent mass ratio and $x_{i,\mu} \equiv \left(\frac{m_i(\mu)}{m_W} \right)^2$ is the mass ratio at scale μ , \hat{B} is the scale-independent bag parameter, and P^i are factors containing the RG evolution factors, $[\eta(\mu)]_i$ which are defined as [30]

$$P_{SM}^{VLL} = \left[\eta(3 \text{ GeV}) \right]_{VLL}^{SM} B_1(3 \text{ GeV}), \quad (21)$$

$$P_{SM}^{SLL} = -\frac{5}{8} \left[\eta_{11}(3 \text{ GeV}) \right]_{SLL}^{SM} \left[B_2(3 \text{ GeV}) \right]_{\text{eff}} - \frac{3}{2} \left[\eta_{21}(3 \text{ GeV}) \right]_{SLL}^{SM} \left[B_3(3 \text{ GeV}) \right]_{\text{eff}}, \quad (22)$$

$$P_{SM}^{TLL} = -\frac{5}{8} \left[\eta_{12}(3 \text{ GeV}) \right]_{SLL}^{SM} \left[B_2(3 \text{ GeV}) \right]_{\text{eff}} - \frac{3}{2} \left[\eta_{22}(3 \text{ GeV}) \right]_{SLL}^{SM} \left[B_3(3 \text{ GeV}) \right]_{\text{eff}}. \quad (23)$$

The effective bag parameters $\left[B_i(3 \text{ GeV}) \right]_{\text{eff}}$ are defined as [30]

$$\left[B_i(3 \text{ GeV}) \right]_{\text{eff}} \equiv R(3 \text{ GeV}) B_i(3 \text{ GeV}), \quad (24)$$

where $R(\mu)$ is defined in Eq. (9) and η factors are given by the formulae in Ref. [30] with

$$\eta_4 \equiv \frac{\alpha_s^{(4)}(\mu_b)}{\alpha_s^{(4)}(3 \text{ GeV})}, \quad \eta_5 \equiv \frac{\alpha_s^{(5)}(\mu_W)}{\alpha_s^{(5)}(\mu_b)}. \quad (25)$$

3.2 Result in 2HDM

The Wilson coefficients at the matching scale $\mu_W \sim m_{H^\pm}$ in the 2HDM cases are calculated from the box diagrams in Fig. 1 (b), (c) and (d) which are given by

$$\begin{aligned} C_{III}^{VLL}(\mu_W) = & A_u A_u^* \left[\lambda_c^2 \left(f_4(x_c, x_H) + x_s g_4(x_c, x_H) \right) + \lambda_t^2 \left(f_4(x_t, x_H) + x_s g_4(x_t, x_H) \right) \right. \\ & \left. + 2\lambda_c \lambda_t (f_4(x_c, x_t, x_H) + x_s g_4(x_c, x_t, x_H)) \right] \\ & + A_u A_d^* x_s \left[\lambda_c^2 f_5(x_c, x_H) + \lambda_t^2 f_5(x_t, x_H) + 2\lambda_c \lambda_t f_5(x_c, x_t, x_H) \right] \\ & + A_u^2 A_u^{*2} x_s \left[\lambda_c^2 f_6(x_c, x_H) + \lambda_t^2 f_6(x_t, x_H) + 2\lambda_c \lambda_t f_6(x_c, x_t, x_H) \right], \end{aligned} \quad (26)$$

$$\begin{aligned} C_{III}^{SLL}(\mu_W) = & x_s \left[A_u A_u^* \left(\lambda_c^2 [f_7(x_c, x_H) + g_7(x_c, x_H)] + \lambda_t^2 [f_7(x_t, x_H) + g_7(x_t, x_H)] \right. \right. \\ & \left. \left. + 2\lambda_c \lambda_t [f_7(x_c, x_t, x_H) + g_7(x_c, x_t, x_H)] \right) \right. \\ & + A_u A_d^* \left(\lambda_c^2 f_8(x_c, x_H) + \lambda_t^2 f_8(x_t, x_H) + 2\lambda_c \lambda_t f_8(x_c, x_t, x_H) \right) \\ & + A_u^2 A_u^{*2} \left(\lambda_c^2 f_9(x_c, x_H) + \lambda_t^2 f_9(x_t, x_H) + 2\lambda_c \lambda_t f_9(x_c, x_t, x_H) \right) \\ & + A_u^2 A_d^{*2} \left(\lambda_c^2 f_{10}(x_c, x_H) + \lambda_t^2 f_{10}(x_t, x_H) + 2\lambda_c \lambda_t f_{10}(x_c, x_t, x_H) \right) \\ & \left. - A_u^2 A_u^* A_d^* \left(\lambda_c^2 f_{10}(x_c, x_H) + \lambda_t^2 f_{10}(x_t, x_H) + 2\lambda_c \lambda_t f_{10}(x_c, x_t, x_H) \right) \right], \end{aligned} \quad (27)$$

$$C_{III}^{TLL}(\mu_W) = 0, \quad (28)$$

$$\begin{aligned}
C_C^{VLL}(\mu_W) = & \frac{1}{3}A_u A_u^* \left[\lambda_c^2 \left(f_4(x_c, x_H) + x_s g_4(x_c, x_H) \right) + \lambda_t^2 \left(f_4(x_t, x_H) + x_s g_4(x_t, x_H) \right) \right. \\
& \left. + 2\lambda_c \lambda_t (f_4(x_c, x_t, x_H) + x_s g_4(x_c, x_t, x_H)) \right] \\
& + \frac{1}{3}A_u A_d^* x_s \left[\lambda_c^2 f_5(x_c, x_H) + \lambda_t^2 f_5(x_t, x_H) + 2\lambda_c \lambda_t f_5(x_c, x_t, x_H) \right] \\
& + \frac{11}{18}A_u^2 A_u^{*2} x_s \left[\lambda_c^2 f_6(x_c, x_H) + \lambda_t^2 f_6(x_t, x_H) + 2\lambda_c \lambda_t f_6(x_c, x_t, x_H) \right], \tag{29}
\end{aligned}$$

$$\begin{aligned}
C_C^{SLL}(\mu_W) = & x_s \left[-\frac{5}{12}A_u A_u^* \left(\lambda_c^2 [f_7(x_c, x_H) + g_7(x_c, x_H)] + \lambda_t^2 [f_7(x_t, x_H) + g_7(x_t, x_H)] \right. \right. \\
& \left. \left. + 2\lambda_c \lambda_t [f_7(x_c, x_t, x_H) + g_7(x_c, x_t, x_H)] \right) \right. \\
& - \frac{5}{12}A_u A_d^* \left(\lambda_c^2 f_8(x_c, x_H) + \lambda_t^2 f_8(x_t, x_H) + 2\lambda_c \lambda_t f_8(x_c, x_t, x_H) \right) \\
& - \frac{19}{72}A_u^2 A_u^{*2} \left(\lambda_c^2 f_9(x_c, x_H) + \lambda_t^2 f_9(x_t, x_H) + 2\lambda_c \lambda_t f_9(x_c, x_t, x_H) \right) \\
& - \frac{19}{72}A_u^2 A_d^{*2} \left(\lambda_c^2 f_{10}(x_c, x_H) + \lambda_t^2 f_{10}(x_t, x_H) + 2\lambda_c \lambda_t f_{10}(x_c, x_t, x_H) \right) \\
& \left. \left. + \frac{19}{72}A_u^2 A_u^* A_d^* \left(\lambda_c^2 f_{10}(x_c, x_H) + \lambda_t^2 f_{10}(x_t, x_H) + 2\lambda_c \lambda_t f_{10}(x_c, x_t, x_H) \right) \right] \right], \tag{30}
\end{aligned}$$

$$\begin{aligned}
C_C^{TLL}(\mu_W) = & x_s \left[\frac{1}{16}A_u A_u^* \left(\lambda_c^2 [f_7(x_c, x_H) + g_7(x_c, x_H)] + \lambda_t^2 [f_7(x_t, x_H) + g_7(x_t, x_H)] \right. \right. \\
& \left. \left. + 2\lambda_c \lambda_t [f_7(x_c, x_t, x_H) + g_7(x_c, x_t, x_H)] \right) \right. \\
& + \frac{1}{16}A_u A_d^* \left(\lambda_c^2 f_8(x_c, x_H) + \lambda_t^2 f_8(x_t, x_H) + 2\lambda_c \lambda_t f_8(x_c, x_t, x_H) \right) \\
& + \frac{7}{96}A_u^2 A_u^{*2} \left(\lambda_c^2 f_9(x_c, x_H) + \lambda_t^2 f_9(x_t, x_H) + 2\lambda_c \lambda_t f_9(x_c, x_t, x_H) \right) \\
& + \frac{7}{96}A_u^2 A_d^{*2} \left(\lambda_c^2 f_{10}(x_c, x_H) + \lambda_t^2 f_{10}(x_t, x_H) + 2\lambda_c \lambda_t f_{10}(x_c, x_t, x_H) \right) \\
& \left. \left. - \frac{7}{96}A_u^2 A_u^* A_d^* \left(\lambda_c^2 f_{10}(x_c, x_H) + \lambda_t^2 f_{10}(x_t, x_H) + 2\lambda_c \lambda_t f_{10}(x_c, x_t, x_H) \right) \right] \right]. \tag{31}
\end{aligned}$$

The f_i functions are given in the appendix. Note that the contribution from C^{TLL} is zero for type-III but is not for type-C. After the RG evolution effect has been included, the result is similar to the SM case and can be written as

$$\langle \bar{K}^0 | \mathcal{H}_{\text{eff}} | K^0 \rangle_{III}^{VLL} = \zeta \left[P_{NP}^{VLL} C_{III}^{VLL}(\mu_t) \right], \tag{32}$$

$$\langle \bar{K}^0 | \mathcal{H}_{\text{eff}} | K^0 \rangle_{III}^{SLL} = \zeta \left[P_{NP}^{SLL} C_{III}^{SLL}(\mu_t) \right], \tag{33}$$

$$\langle \bar{K}^0 | \mathcal{H}_{\text{eff}} | K^0 \rangle_{III}^{TLL} = 0, \quad (34)$$

for type-III and

$$\langle \bar{K}^0 | \mathcal{H}_{\text{eff}} | K^0 \rangle_C^{VLL} = \zeta \left[P_{NP}^{VLL} C_C^{VLL}(\mu_t) \right], \quad (35)$$

$$\langle \bar{K}^0 | \mathcal{H}_{\text{eff}} | K^0 \rangle_C^{SLL} = \zeta \left[P_{NP}^{SLL} C_C^{SLL}(\mu_t) \right], \quad (36)$$

$$\langle \bar{K}^0 | \mathcal{H}_{\text{eff}} | K^0 \rangle_C^{TLL} = \zeta \left[P_{NP}^{TLL} C_C^{TLL}(\mu_t) \right], \quad (37)$$

for type-C. The P^i factors are similar to the SM case with different η_5 factor

$$\eta_5 \equiv \frac{\alpha_s^{(5)}(\mu_t)}{\alpha_s^{(5)}(\mu_b)}. \quad (38)$$

Note that the matching scale for the 2HDMs is changed to $\mu_t \sim m_t$, as the η factor responsible for the evolution from m_{H^\pm} scale to m_t scale is approximately equal to 1, we have neglected the evolution from m_{H^\pm} scale to m_t scale.

After the scale running via RG evolution, the matrix element $\langle \bar{K}^0 | \mathcal{H}_{\text{eff}} | K^0 \rangle$ from the SM and the 2HDMs can be summed directly and can be written as

$$\langle \bar{K}^0 | \mathcal{H}_{\text{eff}} | K^0 \rangle^i = \langle \bar{K}^0 | \mathcal{H}_{\text{eff}} | K^0 \rangle_{SM}^i + \langle \bar{K}^0 | \mathcal{H}_{\text{eff}} | K^0 \rangle_{NP}^i \quad (39)$$

where i is the operator label whereas NP labels the type of the 2HDMs.

4 Numerical results and discussion

Values of the relevant input parameters used throughout this paper are shown in Tab. 2. We use $N_f = 2 + 1$ as a number of effective flavor for the values which are calculated from lattice calculation [33]. Besides, we also use a Mathematica package called *RunDec* [38] to calculate the running coupling constant and the running quark mass at two loops level. At this point, we can calculate the numerical results of Δm_K and ϵ_K in the SM case which are listed in Tab. 1.

We make some comments on the SM results:

1. Δm_K without the corrections from the mass of external strange quark, x_s , and the LD contribution, agrees well with the literature [39].

Corrections Observables	None	LD	x_s	LD, x_s
$(\Delta m_K)_{\text{SM}} (\times 10^{-15} \text{ GeV})$	3.109(1.258)	3.458(1.258)	3.321(1.258)	3.670(1.258)
$\frac{(\Delta m_K)_{\text{SM}}}{(\Delta m_K)_{\text{exp}}}$	89.24%	99.24%	95.34%	105.34%
$(\epsilon_K)_{\text{SM}} (\times 10^{-3})$	$2.219^{+0.309}_{-0.294}$	$2.086^{+0.294}_{-0.280}$	$2.218^{+0.309}_{-0.294}$	$2.085^{+0.294}_{-0.280}$
$\frac{(\epsilon_K)_{\text{SM}}}{(\epsilon_K)_{\text{exp}}}$	99.61%	93.63%	99.55%	93.58%

Table 1: Theoretical predictions on Δm_K and ϵ_K with different corrections in the SM and the ratios of these values with their experimental values. In the table, “None” denotes that the mass and momentum of external strange quark are ignored and the LD contribution has not been considered, either.

2. The corrections from x_s to Δm_K and ϵ_K are 6.83% and -0.06%, respectively. Note that the correction to Δm_K is in the same order as the literature [29]. Moreover, the contribution from the LD part are 11.20% and -6% to Δm_K and ϵ_K , respectively.
3. As the x_s correction can be precisely calculated, we consider the x_s correction both on Δm_K and on ϵ_K , especially, the x_s correction is not too small as for Δm_K . Besides, we also consider the LD contribution to ϵ_K but not to Δm_K in this work, since the LD contribution to Δm_K can not be precisely calculated.

One can see it clearly from Tab. 1 that there is no significant deviation between the SM predictions and the experimental data for the two observables, especially for ϵ_K . Therefore, the two observables are expected to put strong constraints on the parameter spaces of the type-III and type-C 2HDMs. In this literature, the relevant parameters are the two Yukawa couplings $A_{u,d}$ and the charged-Higgs mass m_{H^\pm} . In the case of complex couplings, $|A_u|$ and $A_u A_d^* = |A_u A_d^*| e^{i\theta}$ can be chosen as the independent variables, with θ being the relative phase between A_u and A_d^* . For the parameter $|A_u|$, an upper bound can be obtained from the $Z \rightarrow b\bar{b}$ decay [20], while the parameter A_d is much less constrained phenomenologically [20, 22].

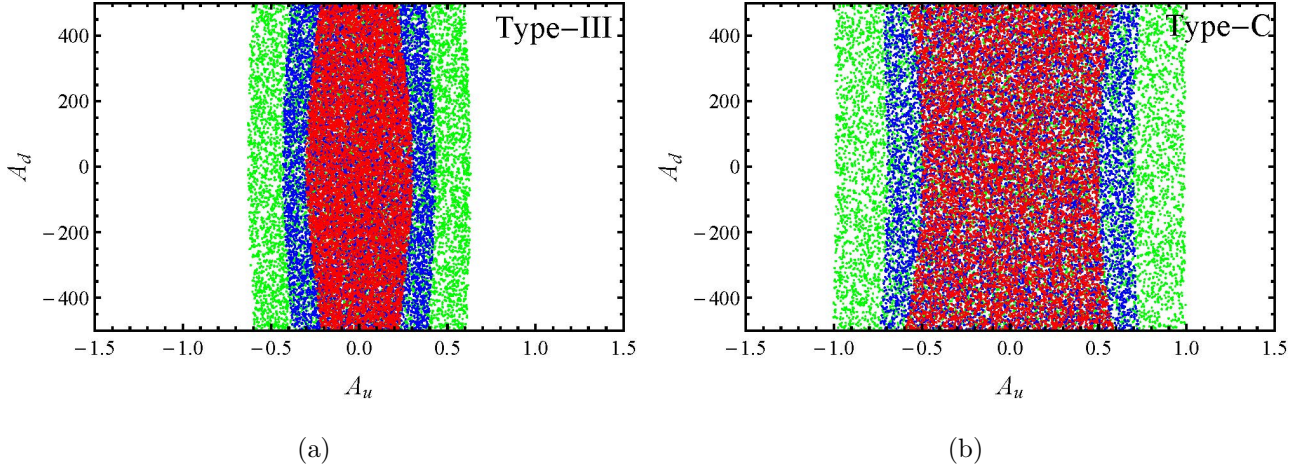


Figure 2: Allowed parameter spaces for A_u and A_d in the case of real coupling for type-III and type-C. The regions are obtained from the combined constraint from Δm_K and ϵ_K . The red, blue and green regions represent the result with m_{H^\pm} at 100, 250 and 500 GeV, respectively.

However, the perturbation theory requires that the coupling cannot be too large. As for the mass of charged Higgs, the lower bound $m_{H^\pm} > 78.6$ GeV (95% CL) [40] has been given by LEP, which is obtained under the assumption that H^\pm decays mainly into fermions without any specific Yukawa structure. Besides, direct searches for H^\pm are also performed by the Tevatron [41], ATLAS [42] and CMS [43, 44], among which most constraints depend strongly on the Yukawa structure. In this literature, we generate randomly numerical points for the parameters as [27, 45]

$$|A_u| \in [0, 3], \quad |A_d| \in [0, 500], \quad \theta \in [-\pi, \pi], \quad m_{H^\pm} = 100, 250, 500 \text{ GeV}. \quad (40)$$

Taking $m_{H^\pm} = 500$ GeV as a benchmark, we explore Wilson coefficients of each operator at the scale $\mu = m_{H^\pm}$ or approximately at $\mu = m_t$,

$$C_{III}^{VLL} \times 10^9 = (41.28 - 42.15i)|A_u|^2 + (6.97 - 7.19i)|A_u|^4 + 10^{-4} \cdot (5.33 - 0.05i)A_u A_d^*, \quad (41)$$

$$C_{III}^{SLL} \times 10^{15} = (3.28 - 3.29i)|A_u|^2 - (0.09 - 0.09i)|A_u|^4 - (308.73 - 25.25i)A_u A_d^* \\ + (0.45 - 0.46i)|A_u|^2 A_u A_d^* - (0.45 - 0.46i)(A_u A_d^*)^2, \quad (42)$$

$$C_C^{VLL} \times 10^9 = (13.76 - 14.05i)|A_u|^2 + (4.26 - 4.39i)|A_u|^4 + 10^{-4} \cdot (1.78 - 0.02i)A_u A_d^*, \quad (43)$$

$$C_C^{SLL} \times 10^{15} = -(1.37 - 1.37i)|A_u|^2 + (0.02 - 0.02i)|A_u|^4 + (128.64 - 10.52i)A_u A_d^* - (0.12 - 0.12i)|A_u|^2 A_u A_d^* + (0.12 - 0.12i)(A_u A_d^*)^2, \quad (44)$$

$$C_C^{TLL} \times 10^{16} = (2.05 - 2.06i)|A_u|^2 - (0.06 - 0.06i)|A_u|^4 - (192.96 - 15.78i)A_u A_d^* + (0.32 - 0.33i)|A_u|^2 A_u A_d^* - (0.32 - 0.33i)(A_u A_d^*)^2. \quad (45)$$

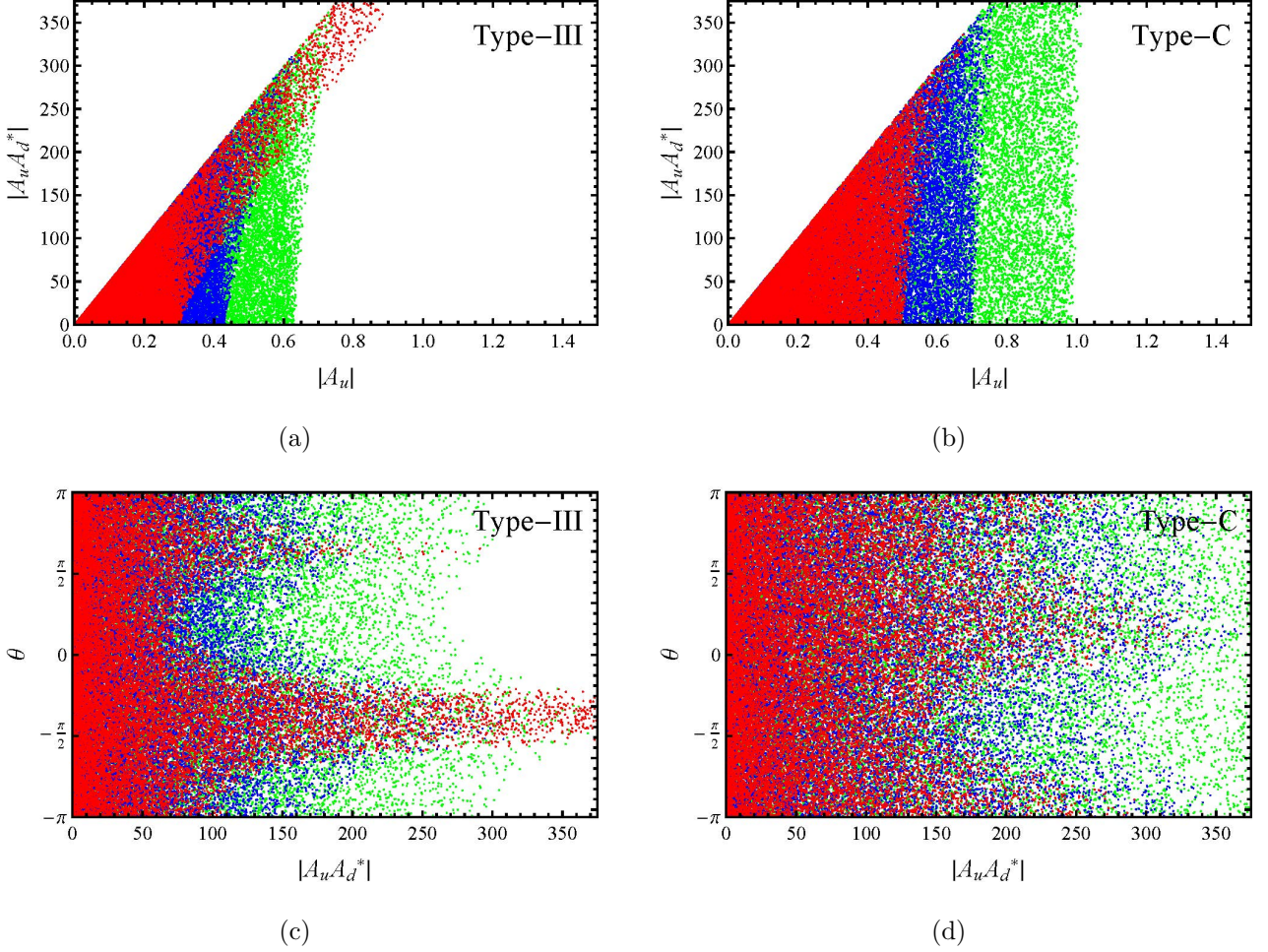


Figure 3: Allowed parameter spaces for $|A_u|$, $|A_u A_d^*|$ and θ in the case of complex coupling for type-III and type-C. The exclusion region in $|A_u A_d^*|$ comes from the constraint on $|A_d|$. The other details are the same as in Fig. 2.

From the above numerical results, we make some observations:

1. The dominant contribution to the effective Hamiltonian (6) comes from Q^{VLL} in both type-III and type-C due to the x_s suppression in Q^{SLL} and Q^{TLL} . Moreover, the terms with $A_u A_d^*$ in Q^{VLL} are small terms of order $\mathcal{O}(10^{-4})$ compared to that with $|A_u|$.

Table 2: Input parameters

General [46]	
$m_W = 80.385(15) \text{ GeV}$	$m_Z = 91.1876(21) \text{ GeV}$
$\mu_W = 80.385 \text{ GeV}$	$\mu_t = 163.427 \text{ GeV}^a$
$G_F = 1.1663787(6) \times 10^{-5} \text{ GeV}^{-2}$	
QCD coupling constant	
$\alpha_s(\mu_t) = 0.1086(10)^a$	$\alpha_s(m_Z) = 0.1182(12) [46]$
$\alpha_s(\mu_W) = 0.1205(12)^a$	$\alpha_s(\mu_b) = 0.2243(45)^a$
$\alpha_s(3 \text{ GeV}) = 0.2521^{+0.0058}_{-0.0057}^a$	
Quark masses	
$m_d(2 \text{ GeV}) = 0.0047^{+0.0005}_{-0.0004} \text{ GeV} [46]$	$m_d(3 \text{ GeV}) = 0.0043^{+0.0005}_{-0.0004} \text{ GeV}^a$
$m_s(2 \text{ GeV}) = 0.096^{+0.008}_{-0.004} \text{ GeV} [46]$	$m_s(3 \text{ GeV}) = 0.087^{+0.007}_{-0.004} \text{ GeV}^a$
$m_s(\mu_W) = 0.057^{+0.005}_{-0.002} \text{ GeV}^a$	$m_s(\mu_t) = 0.054^{+0.005}_{-0.002} \text{ GeV}^a$
$m_c(m_c) = 1.27(3) \text{ GeV} [46]$	$m_c(\mu_W) = 0.660(21) \text{ GeV}^a$
$m_c(\mu_t) = 0.623(20) \text{ GeV}^a$	$M_t = 173.21(87) \text{ GeV} [46]$
$m_t(m_t) = 163.427^{+0.828}_{-0.829} \text{ GeV}^a$	$m_t(\mu_W) = 173.276^{+1.590}_{-1.586} \text{ GeV}^a$
CKM [46]	
$\lambda = 0.22506(50)$	$A = 0.811(26)$
$\bar{\rho} = 0.124^{+0.019}_{-0.018}$	$\bar{\eta} = 0.356(11)$
$\rho = 0.127^{+0.019}_{-0.018}$	$\eta = 0.365(11)$
Kaon	
$m_K = 0.497611(13) \text{ GeV} [46]$	$F_K = 0.1562(9) \text{ GeV} [33]$
$\hat{B}_K = 0.7625(97) [33]$	$B_1(3 \text{ GeV}) = 0.519(26) [47]$
$B_2(3 \text{ GeV}) = 0.525(23) [47]$	$B_3(3 \text{ GeV}) = 0.360(16) [47]$
$B_4(3 \text{ GeV}) = 0.981(62) [47]$	$B_5(3 \text{ GeV}) = 0.751(68) [47]$
$\eta_{cc} = 1.87(76) [37]$	$\eta_{tt} = 0.5765(65) [37]$
$\eta_{ct} = 0.496(47) [37]$	
Experimental Value [46]	
$(\Delta m_K)_{\text{exp}} = 3.4839(59) \times 10^{-15} \text{ GeV}$	$(\epsilon_K)_{\text{exp}} = 2.228(11) \times 10^{-3}$

^a This value is calculated with RunDec package [38] at two loops level.

Table 3: The P factors for the SM and the 2HDM case.

SM $^\diamond$	NP $^\clubsuit$
$P_{VLL}^{SM} = 0.436(22)$	$P_{VLL}^{NP} = 0.426(21)$
$P_{SLL}^{SM} = -16.225_{-1.697}^{+2.362}$	$P_{SLL}^{NP} = -17.398_{-1.821}^{+2.534}$
$P_{TLL}^{SM} = -28.570_{-2.256}^{+3.141}$	$P_{TLL}^{NP} = -30.850_{-2.520}^{+3.508}$

*These values have been calculated by (21), (22) and (23) with η -factors from Tab. 4, $[B_2(3 \text{ GeV})]_{\text{eff}} = 15.596_{-2.255}^{+1.620}$, $[B_3(3 \text{ GeV})]_{\text{eff}} = 10.694_{-1.548}^{+1.113}$ and $R(3 \text{ GeV}) = 29.706_{-4.093}^{+2.797}$.

 Table 4: η -factors for $K^0 - \bar{K}^0$ mixing at $\mu_L = 3 \text{ GeV}$

SM $^\diamond$	NP $^\clubsuit$
$[\eta(\mu_L)]_{VLL}^{SM} = 0.841$	$[\eta(\mu_L)]_{VLL}^{NP} = 0.820$
$[\eta_{11}(\mu_L)]_{SLL}^{SM} = 1.676$	$[\eta_{11}(\mu_L)]_{SLL}^{NP} = 1.798$
$[\eta_{12}(\mu_L)]_{SLL}^{SM} = 2.044$	$[\eta_{12}(\mu_L)]_{SLL}^{NP} = 2.352$
$[\eta_{21}(\mu_L)]_{SLL}^{SM} = -0.007$	$[\eta_{21}(\mu_L)]_{SLL}^{NP} = -0.008$
$[\eta_{22}(\mu_L)]_{SLL}^{SM} = 0.539$	$[\eta_{22}(\mu_L)]_{SLL}^{NP} = 0.494$

*These values have been calculated by the formula in Ref. [30] and RunDec package [38].

$^\diamond$ The η -factors for the SM are running from μ_W to 3 GeV.

$^\clubsuit$ The η -factors for the NP are running from μ_t to 3 GeV.

2. The Wilson coefficient C^{VLL} in type-III is a little bigger than that in type-C due to the color factor; and the sign of C^{SLL} in type-C is flipped relative to type-III.
3. There exists an extra operator Q^{TLL} in type-C compared to type-III, and the Wilson coefficient of Q^{TLL} differs with that of Q^{SLL} in sign.

From the current experimental data on Δm_K and ϵ_K , one can constrain the model parameters and even distinguish the two scenarios of 2HDM with MFV. To get the plot for allowed parameter spaces, we do as follows

1. Scanning the Yukawa coupling parameters A_u and A_d also θ for complex coupling randomly within the ranges given by Eq. (40), with m_{H^\pm} fixed at 100, 250 and 500 GeV, respectively.

2. With each set of values for the model parameters, we give the theoretical prediction for Δm_K and ϵ_K , together with the corresponding uncertainty resulted from the input parameters listed in Tab.2. The method of calculating the theoretical uncertainty is the same as Ref. [27].
3. Selecting the points which lead to the range overlapping with the 2σ range of the experimental data.

The allowed spaces for type-III and type-C are shown in Fig. 2 for the real coupling case and Fig. 3 for the complex coupling case, respectively. We make some observations from Fig. 2 for the real couplings

1. In the type-III model, as shown in Fig. 2 (a), A_u is severely constrained due to the agreement between the SM predictions and the experimental data, especially for ϵ_K ; for example $|A_u| < 0.7$ is limited more stringent compared to Ref. [27] with $m_{H^\pm} = 500$ GeV. However, there is almost no constraints on A_d because of the smallness of the coefficient involving A_d , as mentioned earlier.
2. In the type-C model, we also get strong constraint for A_u , but looser than that in the type-III, with the maximum value $|A_u| \approx 1$. The wider allowed range in the type-C comes from the additional color factor. Similar to the type-III, there is almost no constraint on A_d with the same reason as the type-III.
3. The “patterns” of the allowed parameter spaces of these two models are different. For the type-III model, the allowed region looks like “convex lens” while it looks like “concave lens” for type-C, which means the allowed range for $|A_u|$ is smaller with larger $|A_d|$ for the type-III model while the allowed range for $|A_u|$ in type-C can be larger with greater $|A_d|$. The reason is that the dominant contribution to the two observables comes from the operator Q^{VLL} , the Wilson coefficient of which in type-C is smaller than that in type-III. Moreover, the cancellation between the Wilson coefficients Q^{SLL} and Q^{TLL} in the type-C model also reduces the contribution to the observables.

For the complex coupling case, the results in Fig. 3 imply that

1. In the type-III model, the strong correlation between $|A_u|$ and $|A_u A_d^*|$ has been observed in Fig. 3 (a) especially when $m_{H^\pm}=100$ GeV. We also found from Fig. 3 (c) that the large $|A_u A_d^*|$ values are allowed at $\theta \approx \pm\pi/2$ due to the cancellation between the complex terms.
2. In the type-C model, as is shown in Fig. 3 (b) and (d), similar observation can be also made, except for the fact that the constraints on the couplings are a little looser than that in the type-III model. What different from the type-III model is that larger values of $|A_u A_d^*|$ in the $|A_u A_d^*| \sim \theta$ plane occur around $\theta \approx 0$ and $\pm\pi$ resulted from the cancellation between the complex terms.

From the above discussions, one can conclude that the type-III and type-C models present some significantly different behaviors under the experimental constraints from $K^0 - \bar{K}^0$ mixing, but it is hard to distinguish them from each other, especially for the real coupling case or for small $|A_d|$. This difficulty is the result of the significant uncertainties of both theoretical prediction and experimental data. The smaller uncertainties will give us more precise allowed region for these parameters. Moreover, more precise calculation of the LD contribution to both observables is also essential. For example, the LD contribution to Δm_K is around 10% of the experimental value, which puts a considerable effect on the theoretical prediction in the SM and consequentially affects the allowed range for the NP parameters.

5 Conclusion

We have calculated the box diagrams for neutral kaon mixing in both the SM and the 2HDMs case. For the 2HDMs cases, we consider the type-III and type-C models with the MFV hypothesis, in which the second scalar doublet is color-singlet and color-octet, respectively. In our calculation, we also consider the external momentum of the strange quark and keep its mass up to the second order in order to get a gauge-independent result. The weak effective Hamiltonian has been obtained and then the mass difference, Δm_K , and CP-violating parameter, ϵ_K , in neutral kaon mixing have also been derived.

Combining the latest experimental data on $K^0 - \bar{K}^0$ mixing, we then performed a detailed phenomenological analysis of the charged-Higgs effects on this process. The conclusions for this

work can be summarized as follows:

1. At the matching scale, the type-C model presents an extra operator Q^{TLL} compared to the type-III model, while the type-III model also gives a contribution to the Wilson coefficient C_{III}^{TLL} at the low-energy scale induced by RG evolution effect.
2. We get strong constraint on the Yukawa coupling parameter $|A_u|$ in both the real and the complex coupling case, even stronger than that in Ref. [27], while almost no constraint on the other Yukawa coupling $|A_d|$.
3. The allowed parameter spaces for A_u and A_d in the case of real coupling are similar for both types with the wider range in the type-C. If we extend A_d range, however, the allowed region for A_u will be smaller in the type-III and larger in the type-C, like “convex lens” and “concave lens” respectively.
4. In the case of complex coupling, the strong correlation between $|A_u|$ and $|A_u A_d^*|$ is observed, especially for $m_{H^\pm} = 100$ GeV in the type-III model. The phase between $|A_u|$ and $|A_d|$, θ , allows the large values of $|A_u A_d^*|$ at $\theta \approx \pm\pi/2$ in the type-III and $\theta \approx 0$ and $\pm\pi$ in the type-C. This is the result of the cancellation effects between the complex terms.

The differences between the two types of 2HDMs have been observed for the three parameters, A_u , A_d and θ . The distinguishability between these two types depends on the values of the parameters mainly on A_d . The Yukawa coupling, however, cannot be too large and we need smaller uncertainties for both theoretical calculation and experimental data to get more precise allowed region spaces.

Acknowledgements

The work is supported by the National Natural Science Foundation of China (NSFC) under contract Nos. 11675061 and 11435003. XZ is supported by the CCNU-QLPL Innovation Fund (QLPL2015P01).

Appendix A

Coefficient for $K^0 - \bar{K}^0$ mixing

We collect every term of Wilson coefficient for $K^0 - \bar{K}^0$ mixing as functions. Note that the notation $f(x) = \lim_{y \rightarrow x} f(x, y)$ and $f(x, x_H) = \lim_{y \rightarrow x} f(x, y, x_H)$ is applied to every function here.

$$S_0(x_c, x_t) = x_c x_t \left[\frac{(x_c^2 - 8x_c + 4) \ln(x_c)}{4(x_c - 1)^2(x_c - x_t)} - \frac{(x_t^2 - 8x_t + 4) \ln(x_t)}{4(x_t - 1)^2(x_c - x_t)} - \frac{3}{4(x_c - 1)(x_t - 1)} \right] \quad (\text{A1})$$

$$\begin{aligned} f_1(x_c, x_t) = & \frac{\ln(x_t)}{12(x_t - 1)^4(x_c - x_t)^3} \left[x_c^3(x_t^4 - 9x_t^3 + 36x_t^2 - 42x_t + 12) \right. \\ & \left. + x_c^2 x_t(-3x_t^4 + 22x_t^3 - 87x_t^2 + 108x_t - 36) + x_c x_t^3(15x_t^2 - 23x_t + 6) \right] \\ & + \frac{\ln(x_c)}{12(x_c - 1)^4(x_t - x_c)^3} \left[x_t^3(x_c^4 - 9x_c^3 + 36x_c^2 - 42x_c + 12) \right. \\ & \left. + x_t^2 x_c(-3x_c^4 + 22x_c^3 - 87x_c^2 + 108x_c - 36) + x_t x_c^3(15x_c^2 - 23x_c + 6) \right] \\ & - \frac{1}{72(x_c - 1)^3(x_t - 1)^3(x_c - x_t)^2} \left[x_c^5(65x_t^3 - 130x_t^2 + 113x_t - 60) \right. \\ & + x_c^4(-118x_t^4 + 34x_t^3 + 250x_t^2 - 298x_t + 180) \\ & + x_c^3(65x_t^5 + 34x_t^4 + 66x_t^3 - 386x_t^2 + 329x_t - 180) \\ & - 2x_c^2(65x_t^5 - 125x_t^4 + 193x_t^3 - 217x_t^2 + 90x_t - 30) \\ & \left. + x_c x_t(113x_t^4 - 298x_t^3 + 329x_t^2 - 180x_t + 24) - 60(x_t - 1)^3 x_t^2 \right] \quad (\text{A2}) \end{aligned}$$

$$\begin{aligned} f_2(x_c, x_t) = & \frac{x_t}{36(x_c - 1)^3(x_t - 1)^3(x_c - x_t)^2} \left[x_c^5(5x_t^2 - 22x_t + 5) \right. \\ & + 2x_c^4(x_t^3 - x_t^2 + 35x_t - 11) + x_c^3(5x_t^4 - 2x_t^3 - 78x_t^2 - 2x_t + 5) \\ & \left. - 2x_c^2 x_t(11x_t^3 - 35x_t^2 + x_t - 1) + x_c(5x_t^4 - 22x_t^3 + 5x_t^2) \right] \\ & - \frac{x_c^3 x_t \ln(x_c)}{6(x_c - 1)^4(x_c - x_t)^3} \left[3x_c^2(x_t + 1) - x_c(x_t^2 + 10x_t + 1) + 3x_t(x_t + 1) \right] \\ & - \frac{x_t^3 x_c \ln(x_t)}{6(x_t - 1)^4(x_t - x_c)^3} \left[3x_t^2(x_c + 1) - x_t(x_c^2 + 10x_c + 1) + 3x_c(x_c + 1) \right] \quad (\text{A3}) \end{aligned}$$

$$\begin{aligned}
f_3(x_c, x_t) = & -\frac{1}{36(x_c - 1)^3(x_t - 1)^3(x_c - x_t)^2} \left[x_c^5(10x_t^3 - 25x_t^2 + 8x_t - 5) \right. \\
& + x_c^4(-20x_t^4 + 25x_t^3 + 49x_t^2 - 21x_t + 15) \\
& + x_c^3(10x_t^5 + 25x_t^4 - 102x_t^3 + 2x_t^2 + 8x_t - 15) \\
& + x_c^2(-25x_t^5 + 49x_t^4 + 2x_t^3 + 26x_t^2 - 9x_t + 5) \\
& \left. + x_c(8x_t^5 - 21x_t^4 + 8x_t^3 - 9x_t^2 + 2x_t) - 5(x_t - 1)^3x_t^2 \right] \\
& - \frac{\ln(x_t)}{6(x_t - 1)^4(x_c - x_t)^3} \left[x_c^3(3x_t - 1) - x_c^2(x_t^3 + 6x_t^2 - 3x_t) + x_c(3x_t^4 - x_t^3) \right] \\
& - \frac{\ln(x_c)}{6(x_c - 1)^4(x_t - x_c)^3} \left[x_t^3(3x_c - 1) - x_t^2(x_c^3 + 6x_c^2 - 3x_c) + x_t(3x_c^4 - x_c^3) \right] \quad (\text{A4})
\end{aligned}$$

$$\begin{aligned}
f_4(x_c, x_t, x_H) = & \frac{(x_c - 4) x_c^2 x_t \ln(x_c)}{2(x_c - 1)(x_c - x_H)(x_c - x_t)} - \frac{x_c(x_t - 4) x_t^2 \ln(x_t)}{2(x_t - 1)(x_c - x_t)(x_t - x_H)} \\
& - \frac{x_c(x_H - 4) x_H x_t \ln(x_H)}{2(x_H - 1)(x_c - x_H)(x_H - x_t)} \\
& + x_s \left(\frac{x_c^2 x_t \ln(x_c)}{24(x_c - 1)^3(x_c - x_H)^3(x_c - x_t)^3} \left[-3x_c^5(x_H + 2x_t - 7) \right. \right. \\
& + x_c^4(4x_H(4x_t - 3) + x_H^2 + 2x_t^2 + 16x_t - 23) \\
& - x_c^3(x_H^2(6x_t - 7) + x_H(5x_t^2 + 76x_t + 5) + 5x_t^2 + 42x_t - 12) \\
& + x_c^2(x_H^2(x_t^2 + 28x_t + 2) + 8x_H x_t(3x_t + 20) + x_t(13x_t + 12)) \\
& \left. \left. - 3x_c x_H x_t(x_H(x_t + 22) + 17x_t + 20) + 12x_H x_t(x_H(x_t + 2) + x_t) \right] \right. \\
& - \frac{x_c x_t^2 \ln(x_t)}{24(x_t - 1)^3(x_c - x_t)^3(x_t - x_H)^3} \left[x_c^2(x_H^2(x_t^2 - 3x_t + 12) \right. \\
& + x_H(-5x_t^3 + 24x_t^2 - 51x_t + 12) + x_t^2(2x_t^2 - 5x_t + 13)) \\
& - 2x_c(x_H^2(3x_t^3 - 14x_t^2 + 33x_t - 12) + 2x_H x_t(-4x_t^3 + 19x_t^2 - 40x_t + 15) \\
& + x_t^2(3x_t^3 - 8x_t^2 + 21x_t - 6)) + x_t^2(x_H^2(x_t^2 + 7x_t + 2) \\
& \left. \left. - x_H x_t(3x_t^2 + 12x_t + 5) + x_t(21x_t^2 - 23x_t + 12) \right] \right. \\
& - \frac{x_c x_H x_t \ln(x_H)}{24(x_H - 1)^3(x_c - x_H)^3(x_H - x_t)^3} \left[x_c^2(x_H^3(6 - 5x_t) \right. \\
& + x_H^2(2x_t^2 + 16x_t + 13) - 3x_H x_t(2x_t + 21) + x_H^4 + 12x_t(2x_t + 1)) \\
& - x_c(x_H^4(8 - 12x_t) + x_H^3(5x_t^2 + 40x_t + 41) - 4x_H^2(4x_t^2 + 39x_t + 3) \\
& + 3x_H x_t(21x_t + 16) + 3x_H^5 - 12x_t^2) + x_H^2(-3x_H^3(x_t - 6) \\
& \left. \left. + x_H^2(x_t^2 - 8x_t + 2) + x_H x_t(6x_t - 41) + x_t(13x_t + 12) \right] \right] \Bigg)
\end{aligned} \tag{A5}$$

$$\begin{aligned}
g_4(x_c, x_t, x_H) = & -\frac{x_c x_t}{12(x_c - 1)^2(x_c - x_H)^2(x_H - 1)^2(x_c - x_t)^2(x_H - x_t)^2(x_t - 1)^2} \left[\right. \\
& x_c^5 \left((x_t^2 + 4)x_H^3 + (-13x_t^2 + 15x_t - 17)x_H^2 + (4x_t^3 - 4x_t^2 + 12x_t + 3)x_H \right. \\
& \left. + x_t(6x_t^2 - 14x_t + 3) \right) - \left((3x_t^2 - 2x_t + 9)x_H^4 - (2x_t^3 + 11x_t^2 - 22x_t + 24)x_H^3 \right. \\
& + (2x_t^4 - 16x_t^3 - 11x_t^2 + 31x_t - 21)x_H^2 + (4x_t^4 + 11x_t^3 + x_t^2 + 13x_t + 6)x_H \\
& \left. + x_t(14x_t^3 - 23x_t^2 - 12x_t + 6) \right) x_c^4 + x_c^3 \left((x_t^2 + 4)x_H^5 + (23x_t^2 - 25x_t + 17)x_H^4 \right. \\
& + 2(x_t^4 - 32x_t^3 + 14x_t^2 + 22x_t - 35)x_H^3 + 8(2x_t^4 + x_t^3 - 4x_t^2 + 4x_t + 2)x_H^2 \\
& + (4x_t^5 - 11x_t^4 + 8x_t^3 + 35x_t^2 - 24x_t + 3)x_H + x_t(6x_t^4 + 23x_t^3 - 72x_t^2 + 25x_t + 3) \left. \right) \\
& + \left((x_t^3 - 18x_t^2 + 17x_t - 15)x_H^5 + (-3x_t^4 + 23x_t^3 - 22x_t^2 - 2x_t + 19)x_H^4 \right. \\
& + (x_t^5 + 11x_t^4 + 28x_t^3 - 16x_t^2 - 5x_t + 21)x_H^3 \\
& - (13x_t^5 - 11x_t^4 + 32x_t^3 + 16x_t^2 - 5x_t + 15)x_H^2 \\
& \left. - x_t(4x_t^4 + x_t^3 - 35x_t^2 + 30x_t - 15)x_H + x_t^2(-14x_t^3 + 12x_t^2 + 25x_t - 18) \right) x_c^2 \\
& + \left((17x_t^2 - 8x_t + 6)x_H^5 + (2x_t^4 - 25x_t^3 - 2x_t^2 + 2x_t - 12)x_H^4 \right. \\
& + (-22x_t^4 + 44x_t^3 - 5x_t^2 - 8x_t + 6)x_H^3 + x_t(15x_t^4 - 31x_t^3 + 32x_t^2 + 5x_t - 6)x_H^2 \\
& + x_t^2(12x_t^3 - 13x_t^2 - 24x_t + 15)x_H + 3(x_t - 1)^2 x_t^3 \left. \right) x_c \\
& + x_H x_t \left((4x_t^2 - 15x_t + 6)x_H^4 + (-9x_t^3 + 17x_t^2 + 19x_t - 12)x_H^3 \right. \\
& + (4x_t^4 + 24x_t^3 - 70x_t^2 + 21x_t + 6)x_H^2 + x_t(-17x_t^3 + 21x_t^2 + 16x_t - 15)x_H \\
& \left. + 3(x_t - 1)^2 x_t^2 \right) \left. \right] \tag{A6}
\end{aligned}$$

$$\begin{aligned}
f_5(x_c, x_t, x_H) = & -\frac{x_c \ln(x_c)}{4(x_c - 1)^2(x_c - x_H)^2(x_c - x_t)} \left[-x_c^2(6x_H + 11x_t + 6) \right. \\
& + 2x_c \left(x_H(6x_t + 3) + 5x_t \right) + 6x_c^3 - 11x_H x_t \left. \right] + \frac{x_c x_t \ln(x_t)}{4(x_t - 1)^2(x_c - x_t)(x_H - x_t)^2} \\
& \left[x_H(6x_t - 5) + (4 - 5x_t)x_t \right] + \frac{x_c \ln(x_H)}{4(x_H - 1)^2(x_c - x_H)^2(x_H - x_t)^2} \left[\right. \\
& x_c \left(-x_H^2(19x_t + 6) + x_H x_t(12x_t + 17) + 6x_H^3 - 10x_t^2 \right) \\
& + x_H \left(x_H^2(20x_t + 6) - x_H x_t(13x_t + 18) - 6x_H^3 + 11x_t^2 \right) \left. \right] \\
& - \frac{x_c x_t}{4(x_c - 1)(x_H - 1)(x_t - 1)(x_c - x_H)(x_H - x_t)} \left[\right. \\
& x_c(x_H - 2x_t + 1) + x_H x_t - x_H^2 + x_t - 1 \left. \right] \tag{A7}
\end{aligned}$$

$$\begin{aligned}
f_6(x_c, x_t, x_H) = & \frac{x_c^3 x_t \ln(x_c)}{4(x_c - x_H)^2(x_c - x_t)} - \frac{x_c x_t^3 \ln(x_t)}{4(x_c - x_t)(x_H - x_t)^2} \\
& - \frac{x_c x_H x_t \ln(x_H)}{4(x_c - x_H)^2(x_H - x_t)^2} \left[x_c(x_H - 2x_t) + x_H x_t \right] - \frac{x_c x_H x_t}{4(x_c - x_H)(x_H - x_t)} \\
& + x_s \left(\frac{x_c^3 x_t \ln(x_c)}{12(x_c - x_H)^4(x_c - x_t)^3} \left[3x_c^2(x_H + x_t) - x_c(10x_H x_t + x_H^2 + x_t^2) \right. \right. \\
& + 3x_H x_t(x_H + x_t) \left. \right] + \frac{x_c x_t^3 \ln(x_t)}{12(x_c - x_t)^3(x_H - x_t)^4} \left[x_c^2(x_t - 3x_H) \right. \\
& + x_c(10x_H x_t - 3x_H^2 - 3x_t^2) + x_H x_t(x_H - 3x_t) \left. \right] + \frac{x_c x_t \ln(x_H)}{12(x_c - x_H)^4(x_H - x_t)^4} \left[\right. \\
& - 3x_c x_H^4(x_H - 3x_t) + 3x_c^2 x_H x_t^2(x_t - 3x_H) + x_c^3 x_t^2(3x_H - x_t) + x_H^5(x_H - 3x_t) \left. \right] \\
& + \frac{x_c x_t}{72(x_c - x_H)^3(x_c - x_t)^2(x_H - x_t)^3} \left[x_c^4(-22x_H x_t + 5x_H^2 + 5x_t^2) \right. \\
& + x_c^3(70x_H^2 x_t - 2x_H x_t^2 - 22x_H^3 + 2x_t^3) \\
& + x_c^2(-2x_H^3 x_t - 78x_H^2 x_t^2 - 2x_H x_t^3 + 5x_H^4 + 5x_t^4) \\
& + 2x_c x_H x_t(-x_H^2 x_t + 35x_H x_t^2 + x_H^3 - 11x_t^3) + x_H^2 x_t^2(-22x_H x_t + 5x_H^2 + 5x_t^2) \left. \right] \left. \right) \tag{A8}
\end{aligned}$$

$$\begin{aligned}
f_7(x_c, x_t, x_H) = & -\frac{x_c x_t}{12(x_c - 1)^2(x_c - x_H)^2(x_H - 1)^2(x_c - x_t)^2(x_H - x_t)^2(x_t - 1)^2} \left[\right. \\
& \left((x_t^2 - 3x_t + 4)x_H^3 + (-3x_t^3 + 5x_t^2 - 8)x_H^2 + x_t(4x_t^2 - 13x_t + 15)x_H \right. \\
& \left. + x_t^2(3x_t - 5) \right) x_c^5 + \left((3x_t^2 - 4x_t - 3)x_H^4 + x_t(-7x_t^2 + 5x_t + 8)x_H^3 \right. \\
& + (10x_t^4 + x_t^3 - 16x_t^2 - 4x_t + 15)x_H^2 + x_t(-16x_t^3 + 19x_t^2 + 11x_t - 28)x_H \\
& \left. - x_t^2(2x_t^2 + x_t - 9) \right) x_c^4 + \left((-2x_t^2 + 3x_t + 1)x_H^5 + (6x_t^3 - 10x_t^2 + 5x_t + 5)x_H^4 \right. \\
& + (-7x_t^4 + 8x_t^3 + 4x_t^2 - 16x_t - 13)x_H^3 + (-3x_t^5 + x_t^4 - 16x_t^3 + 28x_t^2 + 11x_t - 5)x_H^2 \\
& \left. + x_t(4x_t^4 + 19x_t^3 - 40x_t^2 + 14x_t + 9)x_H + x_t^2(3x_t^3 - x_t^2 - 6x_t - 2) \right) x_c^3 \\
& + \left((-2x_t^3 + 6x_t^2 - 7x_t - 3)x_H^5 + (3x_t^4 - 10x_t^3 + 8x_t^2 + x_t + 4)x_H^4 \right. \\
& + (x_t^5 + 5x_t^4 + 4x_t^3 - 16x_t^2 + 19x_t + 3)x_H^3 + x_t(5x_t^4 - 16x_t^3 + 28x_t^2 - 40x_t - 1)x_H^2 \\
& \left. + x_t^2(-13x_t^3 + 11x_t^2 + 14x_t - 6)x_H + x_t^3(-5x_t^2 + 9x_t - 2) \right) x_c^2 \\
& + x_H x_t \left((3x_t^2 - 7x_t + 10)x_H^4 + (-4x_t^3 + 5x_t^2 + x_t - 16)x_H^3 \right. \\
& + (-3x_t^4 + 8x_t^3 - 16x_t^2 + 19x_t - 2)x_H^2 - x_t(4x_t^2 - 11x_t + 1)x_H \\
& \left. + x_t^2(15x_t^2 - 28x_t + 9) \right) x_c + x_H^2 x_t^2 \left((x_t - 3)x_H^3 + (-3x_t^2 + 5x_t + 4)x_H^2 \right. \\
& \left. + (4x_t^3 - 13x_t + 3)x_H + x_t(-8x_t^2 + 15x_t - 5) \right) \left. \right] \tag{A9}
\end{aligned}$$

$$\begin{aligned}
g_7(x_c, x_t, x_H) = & -\frac{x_c^2 x_t \ln(x_c)}{6(x_c - 1)^3 (x_c - x_H)^3 (x_c - x_t)^3} \left[6x_c^6 - 3x_c^5 (5x_H + 5x_t + 4) \right. \\
& + x_c^4 \left(5x_H (7x_t + 6) + 8x_H^2 + 7x_t^2 + 29x_t + 5 \right) - x_c^3 \left(2x_H^2 (9x_t + 8) \right. \\
& + x_H (16x_t^2 + 68x_t + 13) + x_t (13x_t + 12) \left. \right) + x_c^2 \left(x_H^2 (8x_t^2 + 35x_t + 7) \right. \\
& + x_H x_t (30x_t + 29) + 5x_t^2 \left. \right) - 3x_c x_H x_t \left(5x_H (x_t + 1) + 4x_t \right) + 6x_H^2 x_t^2 \left. \right] \\
& - \frac{x_t^2 x_c \ln(x_t)}{6(x_t - 1)^3 (x_t - x_H)^3 (x_t - x_c)^3} \left[6x_t^6 - 3x_t^5 (5x_H + 5x_c + 4) \right. \\
& + x_t^4 \left(5x_H (7x_c + 6) + 8x_H^2 + 7x_c^2 + 29x_c + 5 \right) - x_t^3 \left(2x_H^2 (9x_c + 8) \right. \\
& + x_H (16x_c^2 + 68x_c + 13) + x_c (13x_c + 12) \left. \right) + x_t^2 \left(x_H^2 (8x_c^2 + 35x_c + 7) \right. \\
& + x_H x_c (30x_c + 29) + 5x_c^2 \left. \right) - 3x_t x_H x_c \left(5x_H (x_c + 1) + 4x_c \right) + 6x_H^2 x_c^2 \left. \right] \\
& + \frac{x_c x_H x_t \ln(x_H)}{6(x_H - 1)^3 (x_c - x_H)^3 (x_H - x_t)^3} \left[x_c^2 \left(-x_H^3 (16x_t + 15) + x_H^2 (7x_t^2 + 29x_t + 5) \right. \right. \\
& - 3x_H x_t (4x_t + 3) + 8x_H^4 + 3x_t^2 \left. \right) + x_c x_H \left(x_H^3 (36x_t + 35) - x_H^2 (16x_t^2 + 68x_t + 13) \right. \\
& + x_H x_t (29x_t + 24) - 18x_H^4 - 9x_t^2 \left. \right) + x_H^2 \left(-18x_H^3 (x_t + 1) + x_H^2 (8x_t^2 + 35x_t + 7) \right. \\
& \left. \left. - x_H x_t (15x_t + 13) + 9x_H^4 + 5x_t^2 \right) \right] \tag{A10}
\end{aligned}$$

$$\begin{aligned}
f_8(x_c, x_t, x_H) = & \frac{x_c x_t}{4(x_c - 1)(x_H - 1)(x_t - 1)(x_c - x_H)(x_H - x_t)} \left[\right. \\
& x_H \left(x_c (x_t - 2) - 2x_t + 1 \right) + x_c x_t + x_H^2 \left. \right] - \frac{x_c^2 \ln(x_c)}{4(x_c - 1)^2 (x_c - x_H)^2 (x_c - x_t)} \left[\right. \\
& - x_c^2 (9x_H + 16x_t + 9) + x_c \left(x_H (17x_t + 9) + 15x_t \right) + 9x_c^3 - 16x_H x_t \left. \right] \\
& + \frac{x_c x_t^2 \ln(x_t)}{4(x_t - 1)^2 (x_c - x_t)(x_H - x_t)^2} \left[x_H (8x_t - 7) + (6 - 7x_t) x_t \right] \\
& + \frac{x_c x_H \ln(x_H)}{4(x_H - 1)^2 (x_c - x_H)^2 (x_H - x_t)^2} \left[\right. \\
& x_c \left(-x_H^2 (26x_t + 9) + 8x_H x_t (2x_t + 3) + 9x_H^3 - 14x_t^2 \right) + x_H \left(9x_H^2 (3x_t + 1) \right. \\
& \left. \left. - x_H x_t (17x_t + 25) - 9x_H^3 + 15x_t^2 \right) \right] \tag{A11}
\end{aligned}$$

$$\begin{aligned}
f_9(x_c, x_t, x_H) = & -\frac{x_c^3 x_t \ln(x_c)}{6(x_c - x_H)^4 (x_c - x_t)^3} \left[3x_c^2 (x_H + x_t) - x_c (10x_H x_t + x_H^2 + x_t^2) \right. \\
& \left. + 3x_H x_t (x_H + x_t) \right] - \frac{x_c x_t^3 \ln(x_t)}{6(x_c - x_t)^3 (x_H - x_t)^4} \left[x_c^2 (x_t - 3x_H) \right. \\
& \left. + x_c (10x_H x_t - 3x_H^2 - 3x_t^2) + x_H x_t (x_H - 3x_t) \right] + \frac{x_c x_t \ln(x_H)}{6(x_c - x_H)^4 (x_H - x_t)^4} \left[\right. \\
& \left. 3x_c x_H^4 (x_H - 3x_t) + 3x_c^2 x_H x_t^2 (3x_H - x_t) + x_c^3 x_t^2 (x_t - 3x_H) + x_H^5 (3x_t - x_H) \right] \\
& - \frac{x_c x_t}{36(x_c - x_H)^3 (x_c - x_t)^2 (x_H - x_t)^3} \left[x_c^4 (-22x_H x_t + 5x_H^2 + 5x_t^2) \right. \\
& + x_c^3 (70x_H^2 x_t - 2x_H x_t^2 - 22x_H^3 + 2x_t^3) \\
& + x_c^2 (-2x_H^3 x_t - 78x_H^2 x_t^2 - 2x_H x_t^3 + 5x_H^4 + 5x_t^4) \\
& \left. + 2x_c x_H x_t (-x_H^2 x_t + 35x_H x_t^2 + x_H^3 - 11x_t^3) + x_H^2 x_t^2 (-22x_H x_t + 5x_H^2 + 5x_t^2) \right] \quad (A12)
\end{aligned}$$

$$\begin{aligned}
f_{10}(x_c, x_t, x_H) = & \frac{x_c^2 x_t \ln(x_c)}{(x_c - x_H)^2 (x_c - x_t)} - \frac{x_c x_t^2 \ln(x_t)}{(x_c - x_t)(x_H - x_t)^2} \\
& + \frac{x_c x_t \ln(x_H)}{(x_c - x_H)^2 (x_H - x_t)^2} \left[x_c x_t - x_H^2 \right] - \frac{x_c x_t}{(x_c - x_H)(x_H - x_t)} \quad (A13)
\end{aligned}$$

References

- [1] G. Aad et al., “Observation of a new particle in the search for the Standard Model Higgs boson with the ATLAS detector at the LHC,” *Physics Letters B*, vol. 716, pp. 1–29, 2012.
- [2] S. Chatrchyan et al., “Observation of a new boson at a mass of 125 GeV with the CMS experiment at the LHC,” *Physics Letters B*, vol. 716, pp. 30–61, 2012.
- [3] M. Carena and H. E. Haber, “Higgs boson theory and phenomenology,” *Progress in Particle and Nuclear Physics*, vol. 50, pp. 63–152, 2003.
- [4] M. Trodden, “Electroweak baryogenesis: A Brief review,” in *Proceedings, 33rd Rencontres de Moriond 98 electroweak interactions and unified theories: Les racs, France, Mar 14-21, 1998*, pp. 471–480, 1998.
- [5] S. Dimopoulos and L. Susskind, “Baryon Asymmetry in the Very Early Universe,” *Physics Letters B*, vol. 81, pp. 416–418, 1979.

- [6] J. M. Cline, “Baryogenesis,” in *Les Houches Summer School - Session 86: Particle Physics and Cosmology: The Fabric of Spacetime Les Houches, France, July 31-August 25, 2006*, 2006.
- [7] T. D. Lee, “A Theory of Spontaneous T Violation,” *Physical Review D*, vol. 8, pp. 1226–1239, 1973.
- [8] N. Cabibbo, “Unitary Symmetry and Leptonic Decays,” *Physical Review Letters*, vol. 10, pp. 531–533, 1963.
- [9] M. Kobayashi and T. Maskawa, “CP Violation in the Renormalizable Theory of Weak Interaction,” *Progress of Theoretical Physics*, vol. 49, pp. 652–657, 1973.
- [10] S. L. Glashow, J. Iliopoulos, and L. Maiani, “Weak Interactions with Lepton-Hadron Symmetry,” *Physical Review D*, vol. 2, pp. 1285–1292, 1970.
- [11] S. L. Glashow and S. Weinberg, “Natural Conservation Laws for Neutral Currents,” *Physical Review D*, vol. 15, p. 1958, 1977.
- [12] A. J. Buras, P. Gambino, M. Gorbahn, S. Jager, and L. Silvestrini, “Universal unitarity triangle and physics beyond the standard model,” *Physics Letters B*, vol. 500, pp. 161–167, 2001.
- [13] A. J. Buras, M. V. Carlucci, S. Gori, and G. Isidori, “Higgs-mediated FCNCs: Natural Flavour Conservation vs. Minimal Flavour Violation,” *The Journal of High Energy Physics*, vol. 10, p. 009, 2010.
- [14] G. D’Ambrosio, G. F. Giudice, G. Isidori, and A. Strumia, “Minimal flavor violation: An Effective field theory approach,” *Nuclear Physics B*, vol. 645, pp. 155–187, 2002.
- [15] E. Cerver and J.-M. Grard, “Minimal violation of flavour and custodial symmetries in a vectophobic Two-Higgs-Doublet-Model,” *Physics Letters B*, vol. 712, pp. 255–260, 2012.
- [16] G. C. Branco, P. M. Ferreira, L. Lavoura, M. N. Rebelo, M. Sher, and J. P. Silva, “Theory and phenomenology of two-Higgs-doublet models,” *Physics Reports*, vol. 516, pp. 1–102, 2012.

- [17] J. F. Gunion, H. E. Haber, G. L. Kane, and S. Dawson, “The Higgs Hunter’s Guide,” *Frontier of Physics*, vol. 80, pp. 1–404, 2000.
- [18] S. Davidson and H. E. Haber, “Basis-independent methods for the two-Higgs-doublet model,” *Physical Review D*, vol. 72, p. 035004, 2005.
- [19] A. V. Manohar and M. B. Wise, “Flavor changing neutral currents, an extended scalar sector, and the Higgs production rate at the CERN LHC,” *Physical Review D*, vol. 74, p. 035009, 2006.
- [20] G. Degrandi and P. Slavich, “QCD Corrections in two-Higgs-doublet extensions of the Standard Model with Minimal Flavor Violation,” *Physical Review D*, vol. 81, p. 075001, 2010.
- [21] A. Pich and P. Tuzon, “Yukawa Alignment in the Two-Higgs-Doublet Model,” *Physical Review D*, vol. 80, p. 091702, 2009.
- [22] X.-Q. Li, Y.-D. Yang, and X.-B. Yuan, “Exclusive radiative B-meson decays within minimal flavor-violating two-Higgs-doublet models,” *Physical Review D*, vol. 89, no. 5, p. 054024, 2014.
- [23] M. I. Gresham and M. B. Wise, “Color octet scalar production at the LHC,” *Physical Review D*, vol. 76, p. 075003, 2007.
- [24] A. Idilbi, C. Kim, and T. Mehen, “Factorization and resummation for single color-octet scalar production at the LHC,” *Physical Review D*, vol. 79, p. 114016, 2009.
- [25] R. Bonciani, G. Degrandi, and A. Vicini, “Scalar particle contribution to Higgs production via gluon fusion at NLO,” *The Journal of High Energy Physics*, vol. 11, p. 095, 2007.
- [26] C. P. Burgess, M. Trott, and S. Zuberi, “Light Octet Scalars, a Heavy Higgs and Minimal Flavour Violation,” *The Journal of High Energy Physics*, vol. 09, p. 082, 2009.
- [27] Q. Chang, P.-F. Li, and X.-Q. Li, “ B_s^0 \bar{B}_s^0 mixing within minimal flavor-violating two-Higgs-doublet models,” *The European Physical Journal C: Particles and Fields*, vol. 75, no. 12, p. 594, 2015.

- [28] J. Ellis, “TikZ-Feynman: Feynman diagrams with TikZ,” *Computer Physics Communications*, vol. 210, pp. 103–123, 2017.
- [29] J. Urban, F. Krauss, and G. Soff, “Influence of external momenta in K^0 anti- K^0 and B^0 anti- B^0 mixing,” *Journal of Physics G: Nuclear and Particle Physics*, vol. 23, pp. L25–L31, 1997.
- [30] A. J. Buras, S. Jager, and J. Urban, “Master formulae for $\Delta F=2$ NLO QCD factors in the standard model and beyond,” *Nuclear Physics B*, vol. 605, pp. 600–624, 2001.
- [31] A. J. Buras, D. Guadagnoli, and G. Isidori, “On ϵ_K Beyond Lowest Order in the Operator Product Expansion,” *Physics Letters B*, vol. 688, pp. 309–313, 2010.
- [32] Z. Ligeti and F. Sala, “A new look at the theory uncertainty of ϵ_K ,” *The Journal of High Energy Physics*, vol. 09, p. 083, 2016.
- [33] S. Aoki et al., “Review of lattice results concerning low-energy particle physics,” *The European Physical Journal C: Particles and Fields*, vol. 77, no. 2, p. 112, 2017.
- [34] T. Inami and C. S. Lim, “Effects of Superheavy Quarks and Leptons in Low-Energy Weak Processes $k(L) \rightarrow \mu$ anti- μ , $K^+ \rightarrow \pi^+$ Neutrino anti-neutrino and $K^0 \leftrightarrow$ anti- K^0 ,” *Progress of Theoretical Physics*, vol. 65, p. 297, 1981.
- [35] A. J. Buras, J.-M. Grard, and W. A. Bardeen, “Large N Approach to Kaon Decays and Mixing 28 Years Later: $\Delta I = 1/2$ Rule, \hat{B}_K and ΔM_K ,” *The European Physical Journal C: Particles and Fields*, vol. 74, p. 2871, 2014.
- [36] A. J. Buras, M. Jamin, and P. H. Weisz, “Leading and Next-to-leading QCD Corrections to ϵ Parameter and $B^0 - \bar{B}^0$ Mixing in the Presence of a Heavy Top Quark,” *Nuclear Physics B*, vol. 347, pp. 491–536, 1990.
- [37] C. Bobeth, A. J. Buras, A. Celis, and M. Jung, “Patterns of Flavour Violation in Models with Vector-Like Quarks,” *The Journal of High Energy Physics*, vol. 04, p. 079, 2017.
- [38] K. G. Chetyrkin, J. H. Kuhn, and M. Steinhauser, “RunDec: A Mathematica package for running and decoupling of the strong coupling and quark masses,” *Computer Physics Communications*, vol. 133, pp. 43–65, 2000.

- [39] J. Brod and M. Gorbahn, “Next-to-Next-to-Leading-Order Charm-Quark Contribution to the CP Violation Parameter ϵ_K and ΔM_K ,” *Physical Review Letters*, vol. 108, p. 121801, 2012.
- [40] G. Abbiendi et al., “Search for Charged Higgs bosons: Combined Results Using LEP Data,” *The European Physical Journal C: Particles and Fields*, vol. 73, p. 2463, 2013.
- [41] P. Gutierrez, “Review of charged Higgs searches at the Tevatron,” *PoS*, vol. CHARGED2010, p. 004, 2010.
- [42] G. Aad et al., “Search for a Charged Higgs Boson Produced in the Vector-Boson Fusion Mode with Decay $H^\pm \rightarrow W^\pm Z$ using pp Collisions at $\sqrt{s} = 8$ TeV with the ATLAS Experiment,” *Physical Review Letters*, vol. 114, no. 23, p. 231801, 2015.
- [43] CMS Collaboration, “Search for H^\pm to $c\bar{s}$ decay,” *CMS-PAS-HIG-13-035*, 2014.
- [44] CMS Collaboration, “Search for charged Higgs bosons with the H^\pm to $\tau \nu$ decay channel in the fully hadronic final state at $\sqrt{s} = 8$ TeV,” *CMS-PAS-HIG-14-020*, 2014.
- [45] V. Khachatryan et al., “Search for a charged Higgs boson in pp collisions at $\sqrt{s} = 8$ TeV,” *The Journal of High Energy Physics*, vol. 11, p. 018, 2015.
- [46] C. Patrignani et al., “Review of Particle Physics,” *Chinese Physics C*, vol. 40, no. 10, p. 100001, 2016.
- [47] B. J. Choi et al., “Kaon BSM B-parameters using improved staggered fermions from $N_f = 2 + 1$ unquenched QCD,” *Physical Review D*, vol. 93, no. 1, p. 014511, 2016.